

# S-Se-S type molecule: A bactericidal promoter against H<sub>2</sub>S-induced antibiotic resistance

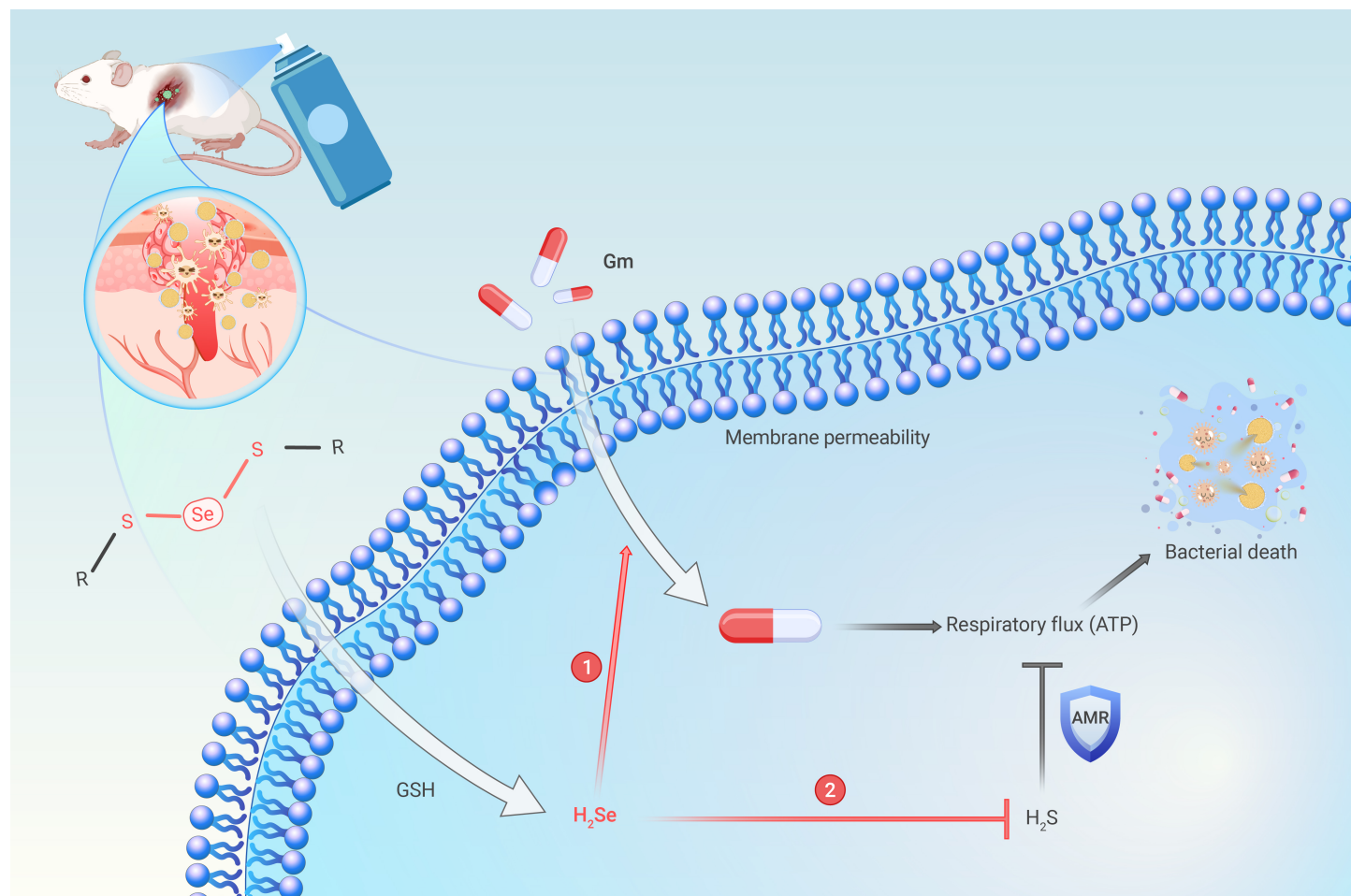
Mengnan Liu,<sup>1,3</sup> Fanqiang Bu,<sup>1,3</sup> Guofeng Li,<sup>1</sup> Wensheng Xie,<sup>1,\*</sup> Huaping Xu,<sup>2,\*</sup> and Xing Wang<sup>1,\*</sup>

\*Correspondence: xws@mail.buct.edu.cn (W.X.); xuhuaping@mail.tsinghua.edu.cn (H.X.); wangxing@mail.buct.edu.cn (X.W.)

Received: April 22, 2024; Accepted: May 27, 2024; Published Online: June 18, 2024; <https://doi.org/10.59717/j.xinn-life.2024.100076>

© 2024 The Author(s). This is an open access article under the CC BY-NC-ND license (<http://creativecommons.org/licenses/by-nc-nd/4.0/>).

## GRAPHICAL ABSTRACT



## PUBLIC SUMMARY

- A unique and stable S-Se-S molecule structure (Se-Acid) was first synthesized and verified.
- A clear reaction mechanism was illustrated about the triggered release of H<sub>2</sub>Se from Se-Acid by glutathione.
- H<sub>2</sub>Se relieved antibiotic resistance through promoting membrane permeability and reactivating respiratory flux.
- S-Se-S type molecule could play key role for addressing the challenge of H<sub>2</sub>S-induced antibiotic resistance.



# S-Se-S type molecule: A bactericidal promoter against H<sub>2</sub>S-induced antibiotic resistance

Mengnan Liu,<sup>1,3</sup> Fanqiang Bu,<sup>1,3</sup> Guofeng Li,<sup>1</sup> Wensheng Xie,<sup>1,\*</sup> Huaping Xu,<sup>2,\*</sup> and Xing Wang<sup>1,\*</sup>

<sup>1</sup>State Key Laboratory of Organic-Inorganic Composites, Beijing Laboratory of Biomedical Materials, School of Life Science and Technology, Beijing University of Chemical Technology, Beijing 100029, China

<sup>2</sup>Key Lab of Organic Optoelectronics and Molecular Engineering, Department of Chemistry, Tsinghua University, Beijing 100084, China

<sup>3</sup>These authors contributed equally

\*Correspondence: [xws@mail.buct.edu.cn](mailto:xws@mail.buct.edu.cn) (W.X.); [xuhuaping@mail.tsinghua.edu.cn](mailto:xuhuaping@mail.tsinghua.edu.cn) (H.X.); [wangxing@mail.buct.edu.cn](mailto:wangxing@mail.buct.edu.cn) (X.W.)

Received: April 22, 2024; Accepted: May 27, 2024; Published Online: June 18, 2024; <https://doi.org/10.59717/j.xinn-life.2024.100076>

© 2024 The Author(s). This is an open access article under the CC BY-NC-ND license (<http://creativecommons.org/licenses/by-nc-nd/4.0/>).

Citation: Liu M., Bu F., Li G., et al., (2024). S-Se-S type molecule: A bactericidal promoter against H<sub>2</sub>S-induced antibiotic resistance. *The Innovation Life* **2**(3): 100076.

The hydrogen sulfide (H<sub>2</sub>S)-induced defense system is a crucial bacterial pathway that leads to antibiotic resistance. Herein, a unique S-Se-S molecule, namely, 2,2'-(selenobis(sulfanediy))diacetic acid (Se-Acid), is first reported to relieve H<sub>2</sub>S-induced antibiotic resistance by acting as a hydrogen selenide (H<sub>2</sub>Se) donor. The S-Se-S molecular structure was formed using the carboxyl terminal as an electron acceptor. After being endocytosed by cells, Se-Acid effectively released H<sub>2</sub>Se molecules by reacting with glutathione (GSH). The released H<sub>2</sub>Se increased the endocytosis of antibiotics by promoting bacterial membrane permeability. Moreover, H<sub>2</sub>Se effectively reactivated the bacterial respiratory flux by functioning as an H<sub>2</sub>S disguiser. The synergistic effect of Se-Acid and Gentamicin (Gm) on H<sub>2</sub>S-induced antibiotic-resistant MRSA was proven on MRSA<sup>S+</sup> wound infection model. Our results establish S-Se-S type molecules as potential tools for addressing the challenge of H<sub>2</sub>S-induced antibiotic resistance and reducing the risk of antibiotic resistance.

## INTRODUCTION

Antibiotic resistance is a widespread and difficult-to-treat public health emergency that is projected to cause the deaths of 10 million people annually by the year 2050.<sup>1,2</sup> Antibiotic resistance is caused by the survival mechanisms which are used by pathogens to circumvent the effects of drugs.<sup>3,4</sup> Bacteria have developed various mechanisms of antibiotic resistance, including reduced permeability, active antibiotic transport, target site modification and protection, drug inactivation, target bypass, and transient slowing of metabolism.<sup>5-7</sup> One particularly important defense mechanism is the production of hydrogen sulfide (H<sub>2</sub>S), which strongly protects bacteria against the toxicity of many clinically used antibiotics and confers multidrug resistance by mitigating antibiotic-triggered oxidative stress.<sup>8-11</sup> Therefore, inhibiting this "gaskeeper" has been demonstrated to be an effective strategy for enhancing the killing of resistant bacteria by antibiotics. For instance, E. Nudler et al. designed an inhibitor of cystathionine  $\gamma$ -lyase (the primary generator of H<sub>2</sub>S in bacteria) to successfully potentiate the bactericidal effects of antibiotics against both *S. aureus* and *P. aeruginosa*.<sup>12</sup> However, genomic organization strategies based on genetic tools are complicated and costly. Thus, a novel strategy using an adjuvant drug to relieve global patterns of H<sub>2</sub>S-induced resistance is critical and essential for the reactivation of clinical antibiotics as well as for the design of novel sensitive drugs.<sup>13-15</sup>

Interestingly, sulfur (S) and selenium (Se), which are congeners in the periodic table, exhibit similar physicochemical properties.<sup>16-18</sup> S is a key component of most relevant enzymes or proteins in bacteria, while Se is not.<sup>19,20</sup> We wondered whether hydrogen selenium (H<sub>2</sub>Se) could relieve the antibiotic resistance induced by H<sub>2</sub>S by acting as a H<sub>2</sub>S disguiser. To investigate this, the design of an effective H<sub>2</sub>Se donor is key, because in practice, H<sub>2</sub>Se is difficult to utilize in its gas state and traditional selenates are not stable during delivery. Moreover, excessive H<sub>2</sub>Se may cause bacterial damage such as selenosis.<sup>21</sup> Luckily, well-defined H<sub>2</sub>Se donors with specific stimulus-response properties will endow them with controllable releasing performances to avoid adverse effects.<sup>22,23</sup>

Considering that a typical H<sub>2</sub>S donor has an organic trisulfide structure and that a triselenide bond is unavailable,<sup>24</sup> a unique S-Se-S molecular structure was first introduced to design a small-molecule H<sub>2</sub>Se donor in our study. Specifically, both oxhydryl (-OH) and carboxyl (-COOH) groups were used as

terminal groups to stabilize the S-Se-S structure by adjusting the electron density. Under the stimulation of glutathione (GSH), the S-Se-S type molecule released H<sub>2</sub>Se via nucleophilic attack to the  $\beta$ -selenium. Then, released H<sub>2</sub>Se acted as a H<sub>2</sub>S disguiser to relieve H<sub>2</sub>S-induced antibiotic resistance by increasing antibiotic endocytosis efficiency and reactivating the bacterial respiratory flux. *In vivo* MRSA<sup>S+</sup> wound infection experiment on mouse model demonstrated the excellent anti-infection effects. Taking the biocompatibility and biosafety into consideration, the design of unique S-Se-S molecular structure may provide a new approach for addressing the challenges of H<sub>2</sub>S-induced antibiotic resistance.

## RESULTS

As shown in Figure 1A, a single-step method was used to prepare 2,2'-(selenobis(sulfanediy))disethanol (Se-Hyd) and 2,2'-(selenobis(sulfanediy))diacetic acid (Se-Acid) under N<sub>2</sub> protection. To evaluate the structural stability of the two H<sub>2</sub>Se donors, a density functional theory calculation was conducted (Figures 1B-D). Evidence has shown that Se-Acid has a larger electron cloud distribution than Se-Hyd (Figure 1C). The atomic Becke charge differences of Se-S (atom 1-atom 2) and S-C (atom 2-atom 3) were both higher than that of Se-Hyd, indicating that the molecular structure of Se-Acid is more stable than that of Se-Hyd. The <sup>1</sup>H and <sup>77</sup>Se NMR spectra of Se-Hyd and Se-Acid directly demonstrated the successful formation of the S-Se-S molecular structure (Figures S1, S2), which was further confirmed by the XPS survey spectra and the relevant S 2p and Se 3d peaks (Figure S3). The mass spectra revealed that the molecular weights of Se-Hyd and Se-Acid were 256.2639 and 262.1032, respectively (Figure S4), and these results are consistent with the theoretical calculations. Furthermore, the stability data (Figures 1E, F) of two H<sub>2</sub>Se donors in aqueous solution revealed that Se-Hyd rapidly decomposed within 30 min, while Se-Acid remained relatively stable for up to 46 h; these results were consistent with the calculation results. Therefore, Se-Acid was chosen as the H<sub>2</sub>Se donor for subsequent evaluation.

First, the *in vitro* release of H<sub>2</sub>Se in response to GSH stimulation was measured. As shown in Figure 2A, when exposed to GSH, two types of nucleophilic attack occurred.<sup>25</sup> For example, attachment to the  $\beta$ -selenium of the S-Se-S donor produced TGA-GSH sulfoselenide (TGA-Se-SG) and 2-thioglycolic acid (TGA). TGA-Se-SG further reacted with GSH, leading to the generation of TGA-I and oxidized GSH (GSSG). When TGA-I was triggered by GSH, H<sub>2</sub>Se gas and TGA-SG were successfully released. Finally, TGA-SG transformed into GSSG and TGA. Alternatively, nucleophilic attack of the  $\alpha$ -sulfur directly led to the formation of TGA-I and TGA-SG. A typical ESI(-)-MS spectrum was used to confirm the reaction between Se-Acid and GSH (Figure 2B). Signals corresponding to the reactants, intermediate products, and terminal products were detected. Furthermore, the accumulative release curve showed that H<sub>2</sub>Se was completely released from Se-Acid within 3 h after exposure to GSH (Figure 2C), indicating its great potential as a H<sub>2</sub>Se donor.

The bactericidal effect of Se-Acid was systematically evaluated by incubating methicillin-resistant *Staphylococcus aureus* (MRSA) with Se-Acid. Se-Acid exhibited a low minimum inhibitory concentration (MIC) of ~8  $\mu$ g/mL (Figure 3A, Figures S5A, B), while its byproduct (TGA) had no toxic effect on MRSA even at a high concentration of 24  $\mu$ g/mL (Figure 3B); these results suggested that its antibacterial effects are attributed to the release of H<sub>2</sub>Se. Can Se-Acid and antibiotics exert synergistic bactericidal effects? A checkerboard dilution assay showed that Se-Acid (1 Mg/mL) could effectively reduce

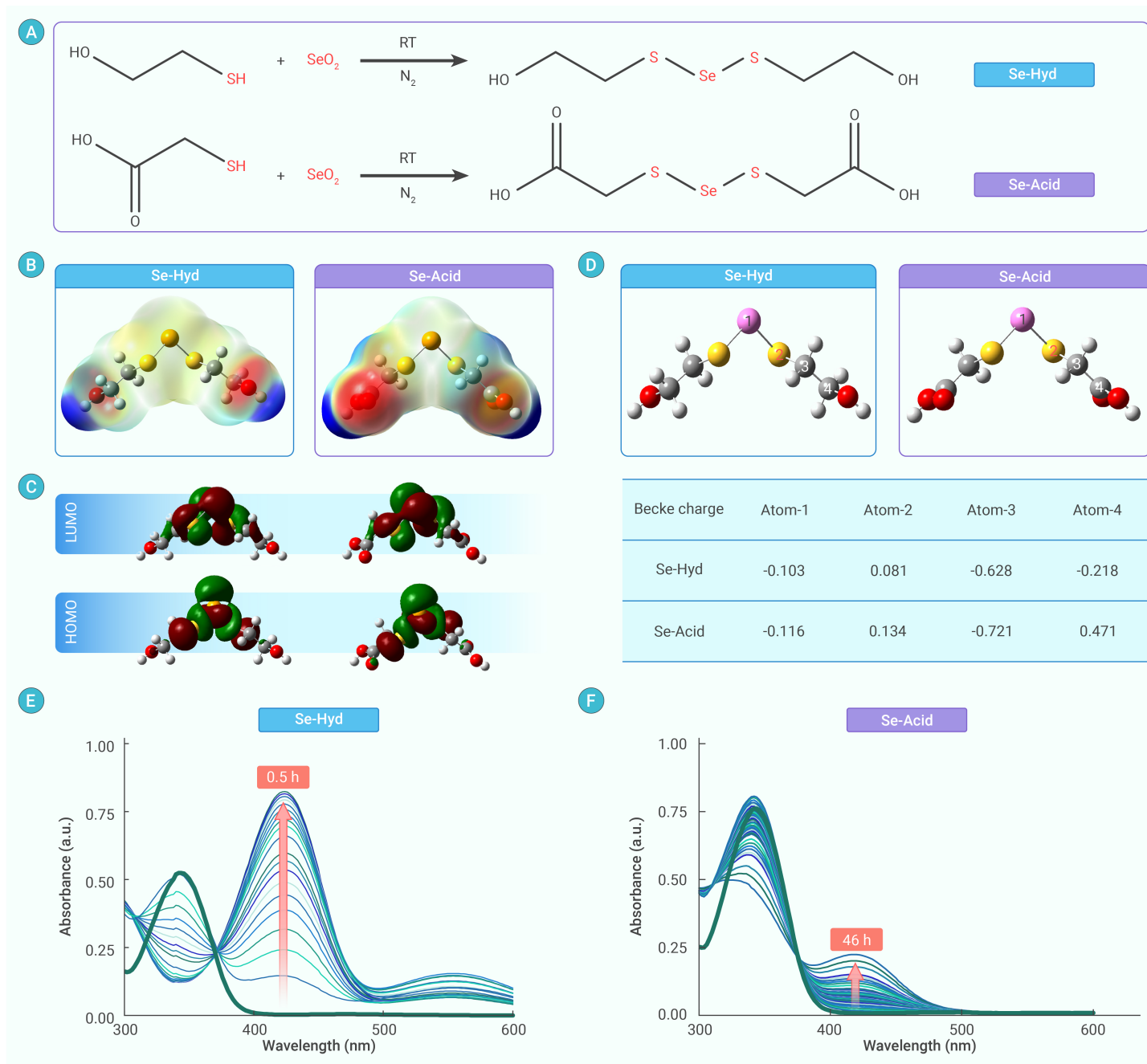


**Figure 1. Synthesis and basic characterization of S-Se-S type molecules** (A) Schematic illustration of the synthesis of Se-Hyd and Se-Acid. (B) Results of structural optimization of the Se-Hyd and Se-Acid molecules using Gaussian simulation calculations. (C) The lowest unoccupied molecular orbitals and highest occupied molecular orbitals of the Se-Hyd and Se-Acid molecules. (D) Calculation of the atomic energy in the Se-Hyd and Se-Acid molecules. (E, F) UV absorption spectra of Se-Hyd and Se-Acid for analyzing the natural release of  $H_2Se$  in aqueous solution.

the MIC of Gm from 512  $\mu\text{g}/\text{mL}$  to 64  $\mu\text{g}/\text{mL}$ , with a fractional inhibitory concentration index (FICI) of 0.25, demonstrating a synergistic effect between Se-Acid and Gm (Figures 3C, D, Figures S5C, D). To further assess the state of MRSA after the combination treatment, the bacteria were cultured for an additional 24 h. Compared to the growth of untreated MRSA, treatment with Gm alone (64  $\mu\text{g}/\text{mL}$ ) or Se-Acid alone (1  $\mu\text{g}/\text{mL}$ ) resulted in limited inhibition of bacterial growth due to the low concentrations (Figure S6). In contrast, combined treatment with Gm and Se-Acid resulted in complete growth inhibition, as confirmed by the standard plate count (Figure S7) and by fluorescence staining (Figure S8) with SYTO 9 (live bacteria) and PI (dead bacteria).

The synergistic effect of Se-Acid and Gm inspired us to evaluate the bactericidal performance of these agents on  $H_2S$ -induced antibiotic-resistant bacteria. First, an antibiotic-resistant MRSA (labeled MRSA<sup>St</sup>) was established by treatment with NaHS according to the literature.<sup>9,12</sup> NaHS had negligible inhibitory effects on MRSA (Figure S9). As shown in Figure 3E, MRSA<sup>St</sup>

exhibited a similar growth rate to that of normal MRSA. Compared to MRSA, MRSA<sup>St</sup> treated with Se-Acid (1  $\mu\text{g}/\text{mL}$ ) showed similar bacterial growth inhibition regardless of the presence of  $H_2S$ . Gm exerted an excellent bactericidal effect on MRSA, but its efficacy on MRSA<sup>St</sup> was significantly decreased due to  $H_2S$ -induced antibiotic resistance. Encouragingly, when Gm was combined with Se-Acid, it exhibited the same bactericidal activity against both MRSA<sup>St</sup> and MRSA, which indicated that Se-Acid could successfully relieve the antibiotic resistance of MRSA<sup>St</sup> that was induced by  $H_2S$ . The above-described bacteria were also collected for further standard plate counting (Figures 3F, G). After treatment with Gm alone, the remaining number of MRSA<sup>St</sup> cells were 8-fold higher than that of MRSA cells. However, after combination treatment with both Gm and Se-Acid, an almost equivalent number of bacteria remained, clearly verifying that Se-Acid eliminated antibiotic resistance. The enhanced bactericidal effects of Se-Acid on Gm-treated MRSA<sup>St</sup> was 18-fold, which was significantly higher than its effects on MRSA (7-fold) (Figure 3G).

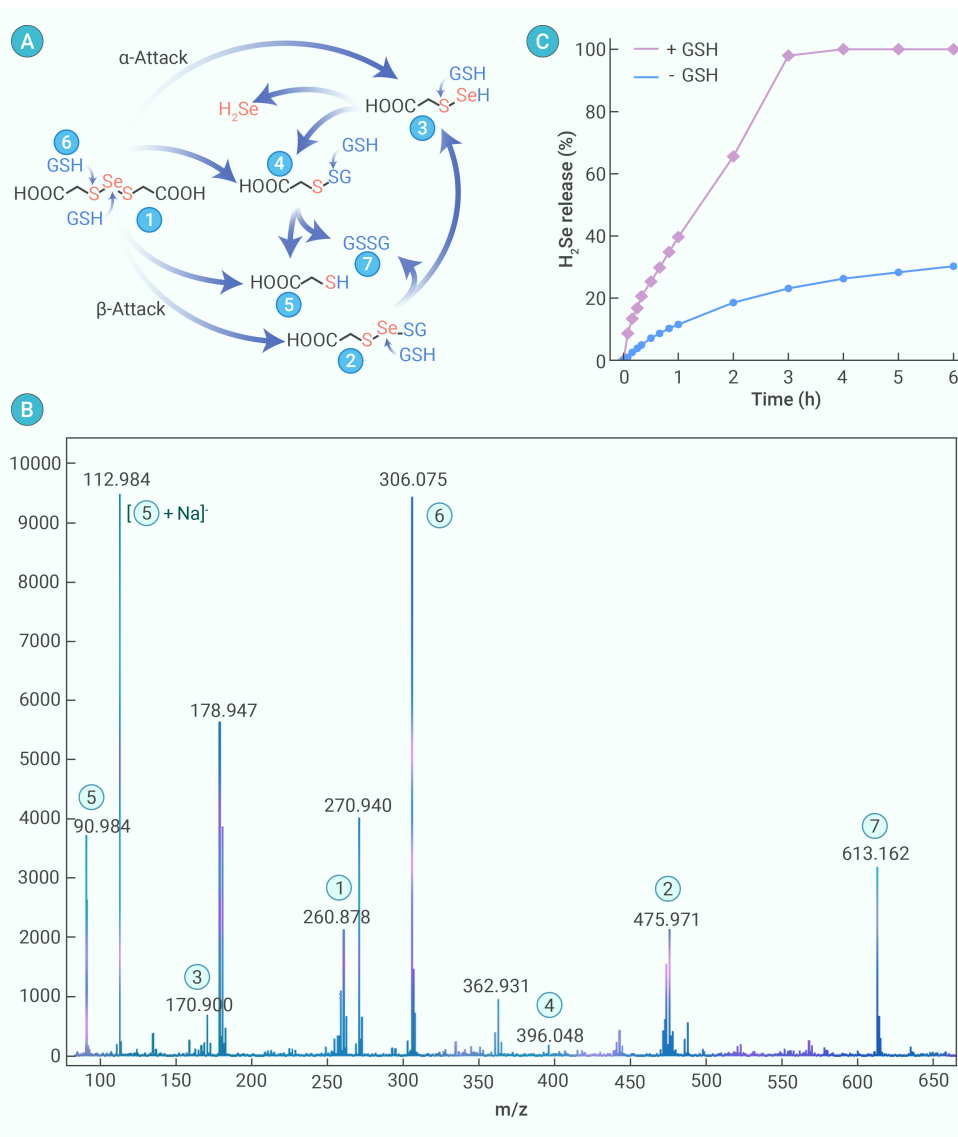


**Figure 2. The mechanisms underlying the release of  $H_2Se$  from Se-Acid in response to GSH (A)** Schematic diagram of donor molecules releasing  $H_2Se$  gas upon GSH exposure. (B) ESI-MS analysis of a reaction containing Se-Acid and GSH at a molar ratio of 1:1. (C) Accumulative release curve of  $H_2Se$  gas from Se-Acid with or without GSH exposure.

To evaluate whether the performance of Se-Acid is universal and applicable beyond Gm, amikacin (Ami), tobramycin (Tob), and ampicillin (Amp) were introduced and systematically assessed. The MICs of Ami, Tob, and Amp against MRSA were 256, 256, and 16  $\mu\text{g}/\text{mL}$ , respectively (Figure S10). Coincubation of Se-Acid with Ami and Tob exerted synergistic effects on MRSA, but no synergistic effect was observed when Se-Acid was combined with Amp (Figures S11, S12). Similarly,  $H_2S$ -induced MRSA<sup>S+</sup> was resistant to Ami and Tob but not to Amp. The targets of Gm, Ami, and Tob are bacterial ribosomes, and the bactericidal effects are attributed to the inhibition of intracellular protein synthesis. However, Amp plays a bactericidal role by preventing the synthesis of bacterial cell walls. It is well known that the  $H_2S$ -induced bacterial defense system protects against antibiotics mainly via the action of specific intracellular enzymes and the maintenance of respiratory flux and redox balance.<sup>10</sup> Thus, this system had a negligible effect on Amp treatment. As shown in Figure S13, Se-Acid effectively relieved the resistance of MRSA<sup>S+</sup> to Ami and Tob, but no efficacy was observed when Se-Acid was combined with Amp, which confirms the difference in bactericidal sites. Thus, these results demonstrate that Se-Acid can effectively relieve  $H_2S$ -induced antibiotic resistance and enhance the bactericidal efficacy of aminoglycoside antibiotics against MRSA<sup>S+</sup>.

How does Se-Acid relieve  $H_2S$ -induced bacterial resistance to antibiotics? We speculated that the mechanism involves two pathways (Figure 4A): (i) the release of  $H_2Se$ , triggered by GSH, increases the bacterial membrane permeability to promote antibiotic endocytosis; and (ii)  $H_2Se$  reactivates the bacterial respiratory flux by acting as an  $H_2S$  disguiser. First, the intracellular Se level was measured after incubation with various concentrations of Se-Acid

(Figure 4B). The concentration-dependent Se level in MRSA<sup>S+</sup> indicated the successful endocytosis of Se-Acid by bacteria. Then, the change of MRSA membrane permeability after treatment with NaHS and Se-Acid demonstrated that MRSA<sup>S+</sup> exhibited a significant decrease in permeability compared with untreated MRSA (Figure S14). In contrast, incubation with Se-Acid significantly increased membrane permeability ( $p = 0.0046$ ) (Figure S15). When MRSA was treated with NaHS and Se-Acid in sequence, the  $H_2S$ -mediated inhibition of membrane permeability was eliminated by the  $H_2Se$  that was released from Se-Acid. This was evident as the optical value at 420 nm returned to normal (Figure 4C, NaHS $\rightarrow$ Se-Acid group). Moreover, when MRSA was first incubated with Se-Acid,  $H_2S$  was unable to inhibit MRSA membrane permeability (Figure 4C, Se-Acid $\rightarrow$ NaHS group). When the concentration of Se-Acid was increased from 0.25 to 1  $\mu\text{g}/\text{mL}$ , the bacterial membrane permeability increased in a concentration-dependent manner (Figure 4D). Furthermore, the MRSA membrane depolarization continuously increased after treatment with a higher concentration of Se-Acid (Figure 4D), which was also confirmed by a decrease in the zeta potential (Figure S15).

Furthermore, adenosine triphosphate (ATP) is the main product of bacterial aerobic respiration and plays a crucial role in bacterial metabolism.<sup>26,27</sup> Thus, the intracellular ATP

concentration could serve as an indicator of changes in bacterial respiratory flux after treatment with various antibiotics. As shown in Figure 4E, when MRSA<sup>S+</sup> was incubated with Gm, intracellular ATP synthesis was strongly blocked due to  $H_2S$ -mediated resistance, which in turn limited the bacterial toxicity of Gm. Notably, combined treatment with Gm and Se-Acid successfully restored the ATP level, indicating that  $H_2Se$  synchronously reactivated the bacterial respiratory flux during Gm treatment and relieved  $H_2S$ -induced bacterial resistance to antibiotics.

To evaluate the *in vivo* bactericidal ability of Se-Acid, an *in vivo* MRSA<sup>S+</sup> wound infection model in mice was constructed, which was described in Figure 5A. Both Gm and Se-Acid were used in the form of spray and the therapeutic effect was monitored and evaluated every two days. As shown in Figure 5B, Gm treated group did not show additional therapeutic effect for MRSA<sup>S+</sup> wound infection compared with PBS group due to the  $H_2S$ -induced antibiotic resistance. Meanwhile, Se-Acid treated group presented finite wound recovery rate (Figures 5C, E). Similar therapeutic effect were obtained on both MRSA and MRSA<sup>S+</sup> wound infection models (Figure S16). The combined treatment with Gm and Se-Acid resulted in optimal efficacy (almost healing on day 10), confirming that Se-Acid relieve  $H_2S$ -induced bacterial resistance to antibiotics *in vivo*. The count statistics of remaining bacteria in infection area after 10 days' treatment showed the number of remaining bacteria decreased to  $10^4$  CFU/mL after combined treatment of Gm and Se-Acid (Figures 5D, F), further revealing the enhanced bactericidal efficacy of Gm assisted by Se-Acid. The Gram staining images of skin tissues around wound infection area presented that a lot of bacteria could be observed in both Gm treated group and Se-Acid treated group (Figure S17).

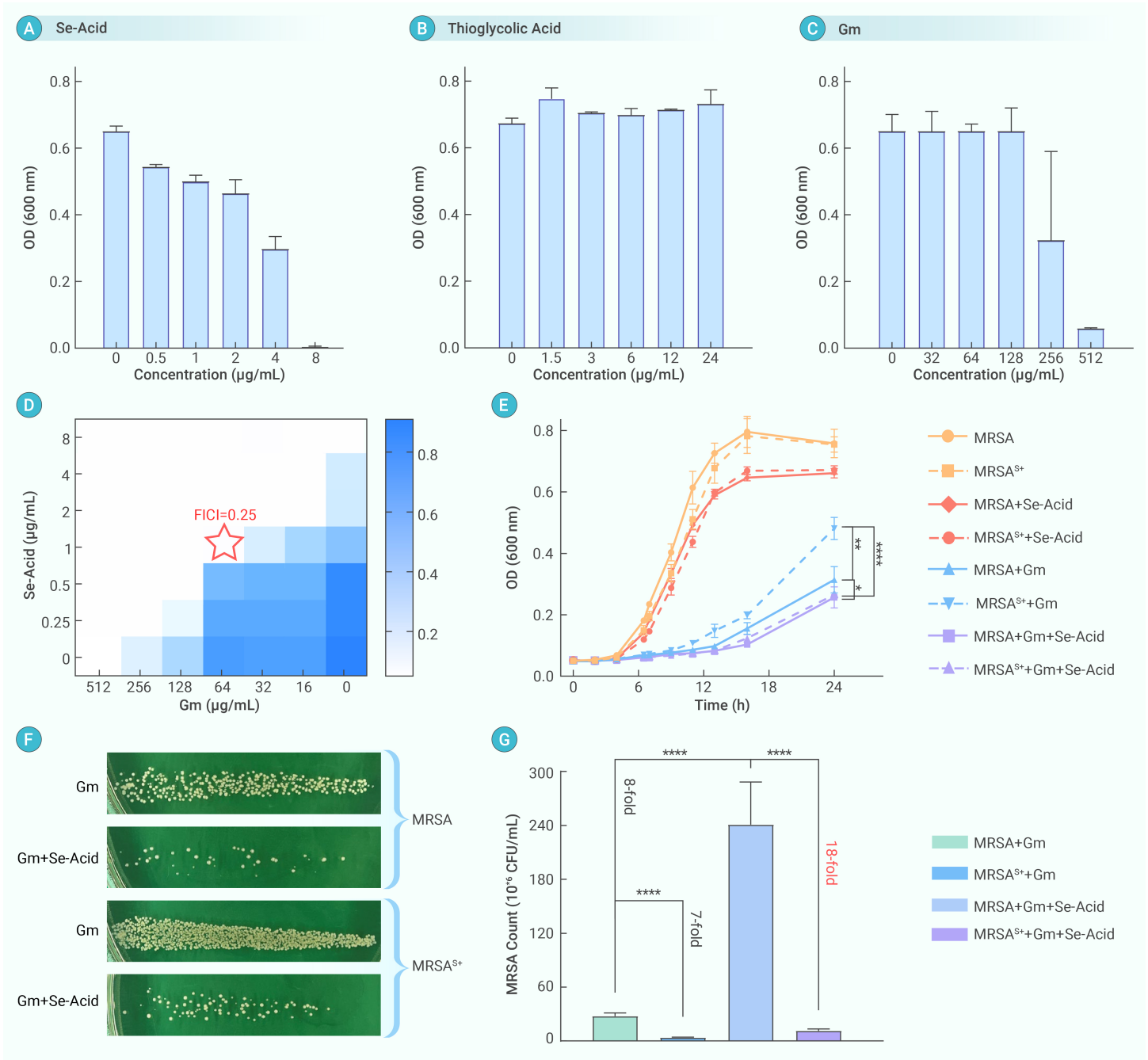


**Figure 3. The synergistic bactericidal effects of Se-Acid and Gm** (A-C) Growth of bacteria after coincubation with different concentrations of Se-Acid, thioglycolic acid or Gm for 24 h. (D) The synergistic effect of Gm and Se-Acid on MRSA cells evaluated using a partial FICI. (E) Growth curves of MRSA and MRSA<sup>S+</sup> treated with Gm alone or in combination with Se-Acid; The colony plate images (F) and colony-forming units quantity statistics (G) of bacteria after treatment with different combinations of Gm (256  $\mu\text{g/mL}$ ) and Se-Acid (1  $\mu\text{g/mL}$ ).

However, only few MRSA<sup>S+</sup> left in skin tissue under the combined treatment of Gm and Se-Acid, visually demonstrating the relieved H<sub>2</sub>S-induced bacterial resistance to antibiotics by our designed H<sub>2</sub>Se donor. Hematoxylin-eosin (H&E) staining images of wound infection area showed obvious epidermis recovery in Se-Acid treated group and Gm/Se-Acid treated group compared with PBS group (Figure S18), which is agreement with the photographs in Figure 5B. Furthermore, the results of Masson staining (Figure S19) showed that a complete subcutaneous tissue appeared in Gm/Se-Acid treated group, demonstrating the optimal therapeutic efficacy. In general, those results mentioned above strongly demonstrated the potential of Se-Acid acting as a H<sub>2</sub>Se donor to relieve the H<sub>2</sub>S-induced bacterial resistance to antibiotics.

Finally, the *in vivo* biosafety of Se-Acid was systematically evaluated through biomedical analysis of blood and pathologic analysis of main organs. As shown in Figure S20, the level of alanine transaminase (ALT), aspartate

aminotransferase (AST), alkaline phosphatase (ALP), albumin (ALB), direct bilirubin (DBIL), total protein (TP), Urea, and creatinine (CREA) in Gm, Se-Acid, and Gm/Se-Acid treated groups showed none significant difference compared with that in PBS group, indicating there was no damage to liver and kidney.<sup>27</sup> H&E staining images (Figure S21) of main organs in all treated groups revealed the biocompatibility and biosafety of Se-Acid, which will guarantee its potential acting as a H<sub>2</sub>Se donor for antibiotic resistance treatment.

## DISCUSSION

In summary, a Se-Acid molecule with a specifically designed S-Se-S type structure was successfully developed to relieve H<sub>2</sub>S-induced antibiotic resistance. Our proof-of-concept results demonstrated that H<sub>2</sub>Se could be rapidly released from Se-Acid upon activation by intracellular GSH. H<sub>2</sub>Se could effec-

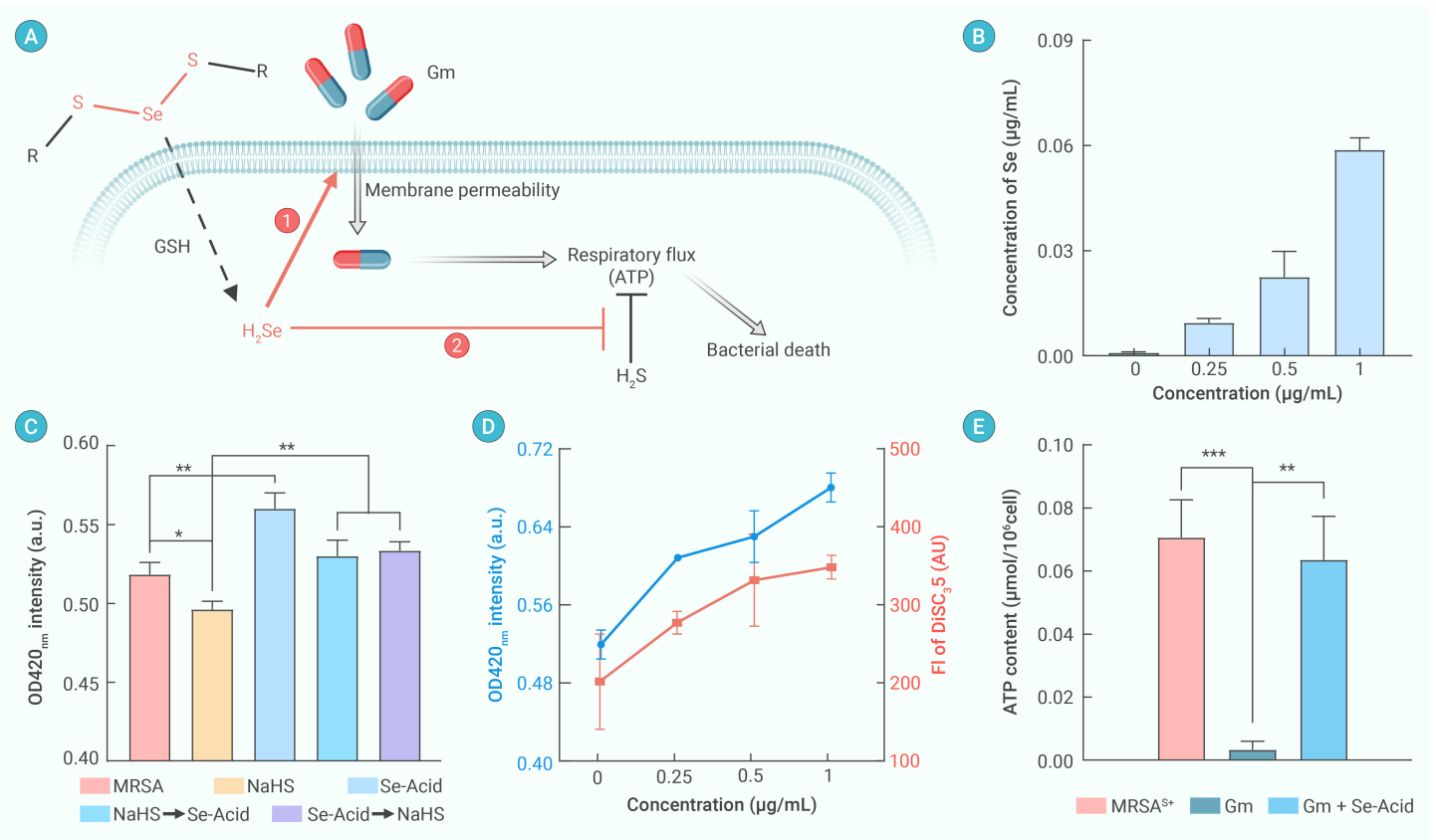


**Figure 4. The mechanism of Se-Acid against H<sub>2</sub>S-induced antibiotic resistance** (A) Schematic illustration of the relevant mechanisms: increasing membrane permeability and reactivating bacterial respiratory flux. (B) The Se level in bacteria after incubation with Se-Acid with different concentrations. (C) Changes in MRSA membrane permeability after various treatments (NaHS, Se-Acid, NaHS→Se-Acid, and Se-Acid→NaHS). (D) Membrane permeability (left) and membrane depolarization (right) of MRSA after incubation with various concentrations of Se-Acid. (E) Changes in the intracellular ATP level of MRSA<sup>+</sup> after different treatments (none, Gm, and Gm + Se-Acid).

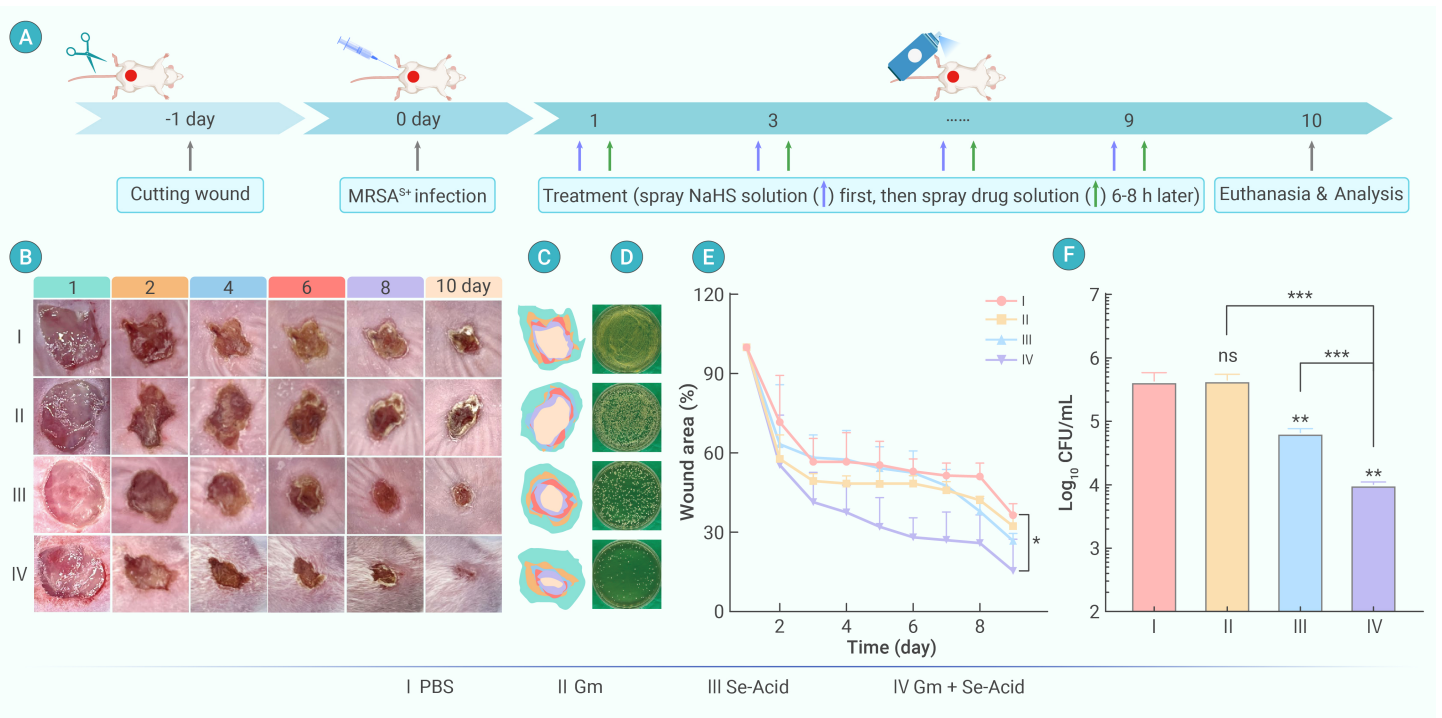


**Figure 5. In vivo anti-infection effects of Se-Acid against H<sub>2</sub>S-induced antibiotic resistance** (A) Schematic diagram of the construction and treatment process of the mouse skin MRSA<sup>+</sup> wound infection model. (B, C) Record photos of wounds (B) and simulate the dynamic healing process of wounds (C) in different experimental groups at different times (I: PBS; II: Gm; III: Se-Acid; IV: Gm + Se-Acid). (D) The colony plate images of remaining bacteria after various treatments. (E) Mean wound area of mice at different stages of various treatments. (F) The colony-forming units quantity statistics of remaining bacteria after various treatments.

tively increase antibiotic endocytosis by promoting bacterial membrane permeability. Meanwhile, H<sub>2</sub>Se acted as an H<sub>2</sub>S disguiser to relieve the activity of antibiotics by reactivating the bacterial respiratory flux. Moreover, excellent anti-infection effects were evaluated on *in vivo* MRSA<sup>S+</sup> wound infection model in mice. Taking the biocompatibility and biosafety into consideration, the design of H<sub>2</sub>Se donors with a S-Se-S molecular structure may provide a new platform for addressing the challenges of H<sub>2</sub>S-induced antibiotic resistance.

In our study, although intracellular H<sub>2</sub>Se exhibited the high efficiency to reactivate the bacterial respiratory flux and alleviate the antibiotic resistance of Gm, the specific mechanism is still unclear and needs further study. For instance, in which way H<sub>2</sub>Se acted as a H<sub>2</sub>S disguiser? What is the key enzymes during the reactivation process? How the intracellular H<sub>2</sub>Se interacts with the key protein? These answers will contribute a better understanding of the antibiotic resistance of bacteria as well as anti-infection therapy.

## REFERENCES

- Darby, E.M., Trampari, E., Siasat, P., et al. (2023). Molecular mechanisms of antibiotic resistance revisited. *Nat. Rev. Microbiol.* **21**: 280–295. DOI: 10.1038/s41579-022-00820-y.
- Larsson, D.G.J., and Flach, C.-F. (2022). Antibiotic resistance in the environment. *Nat. Rev. Microbiol.* **20**: 257–269. DOI: 10.1038/s41579-021-00649-x.
- Stower, H. (2020). Antibiotic tolerance leads to antibiotic resistance. *Nat. Med.* **26**: 163–163. DOI: 10.1038/s41591-020-0778-7.
- Zha, Y., Chen, C., Jiao, Q., et al. (2024). Comprehensive profiling of antibiotic resistance genes in diverse environments and novel function discovery. *The Innovation Life* **2**: 100054. DOI: 10.59717/j.xinn-life.2024.100054.
- Darby, E.M., Trampari, E., Siasat, P., et al. (2023). Molecular mechanisms of antibiotic resistance revisited. *Nat. Rev. Microbiol.* **21**: 280–295. DOI: 10.1038/s41579-022-00820-y.
- Blair, J.M.A., Webber, M.A., Baylay, A.J., et al. (2015). Molecular mechanisms of antibiotic resistance. *Nat. Rev. Microbiol.* **13**: 42–51. DOI: 10.1038/nrmicro3380.
- Michiels, J.E., Van den Bergh, B., Verstraeten, N., et al. (2016). Molecular mechanisms and clinical implications of bacterial persistence. *Drug Resist. Updat.* **29**: 76–89. DOI: 10.1016/j.drug.2016.10.002.
- Kimura, H. (2015). Signaling of hydrogen sulfide and polysulfides. *Antioxid. Redox Signal.* **22**: 347–349. DOI: 10.1089/ars.2014.6082.
- Shatalin, K., Shatalina, E., Mironov, A., et al. (2011). H<sub>2</sub>S: A universal defense against antibiotics in bacteria. *Science* **334**: 986–990. DOI: 10.1126/science.1209855.
- Shukla, P., Khodade, V.S., SharathChandra, M., et al. (2017). "On demand" redox buffering by H<sub>2</sub>S contributes to antibiotic resistance revealed by a bacteria-specific H<sub>2</sub>S donor. *Chem. Sci.* **8**: 4967–4972. DOI: 10.1039/C7SC00873B.
- Kimura H. (2015). Physiological roles of hydrogen sulfide and polysulfides. *Handb. Exp. Pharmacol.* **230**: 61–81. DOI: 10.1007/978-3-319-18144-8\_3.
- Shatalin, K., Nuthanakanti, A., Kaushik, A., et al. (2021). Inhibitors of bacterial H<sub>2</sub>S biogenesis targeting antibiotic resistance and tolerance. *Science* **372**: 1169–1175. DOI: 10.1126/science.abd8377.
- Xie, M., Gao, M., Yun, Y., et al. (2023). Antibacterial nanomaterials: Mechanisms, impacts on antimicrobial resistance and design principles. *Angew.* **62**: e202217345. DOI: 10.1002/anie.202217345.
- Zhang, S., Yang, H., Wang, M., et al. (2023). Immunomodulatory biomaterials against bacterial infections: Progress, challenges, and future perspectives. *The Innovation* **4**: 100503. DOI: 10.1016/j.xinn.2023.100503.
- Makabenta, J.M.V., Nabawy, A., Li, C.-H., et al. (2021). Nanomaterial-based therapeutics for antibiotic-resistant bacterial infections. *Nat. Rev. Microbiol.* **19**: 23–36. DOI: 10.1038/s41579-020-0420-1.
- Cupp-Sutton, K.A., and Ashby, M.T. (2016). Biological chemistry of hydrogen selenide. *Antioxidants* **5**: 42. DOI: 10.3390/antiox5040042.
- Mapelli, V., Hillestrøm, P.R., Patil, K., et al. (2012). The interplay between sulphur and

selenium metabolism influences the intracellular redox balance in *Saccharomyces cerevisiae*. *FEMS Yeast Res.* **12**: 20–32. DOI: 10.1111/j.1567-1364.2011.00757.x.

- Xia, J., Li, T., Lu, C., et al. (2018). Selenium-containing polymers: Perspectives toward diverse applications in both adaptive and biomedical materials. *Macromolecules* **51**: 7435–7455. DOI: 10.1021/acs.macromol.8b01597.
- Kushkevych, I., Cejnar, J., Treml, J., et al. (2020). Recent advances in metabolic pathways of sulfate reduction in intestinal bacteria. *Cells* **9**: 698. DOI: 10.3390/cells9030698.
- Wolf, P.G., Cowley, E.S., Breister, A., et al. (2022). Diversity and distribution of sulfur metabolic genes in the human gut microbiome and their association with colorectal cancer. *Microbiome* **10**: 64. DOI: 10.1186/s40168-022-01242-x.
- Weekley, C.M., and Harris, H.H. (2013). Which form is that? The importance of selenium speciation and metabolism in the prevention and treatment of disease. *Chem. Soc. Rev.* **42**: 8870. DOI: 10.1039/c3cs60272a.
- Kang, X., Huang, H., Jiang, C., et al. (2022). Cysteine-activated small-molecule H<sub>2</sub>Se donors inspired by synthetic H<sub>2</sub>S donors. *J. Am. Chem. Soc.* **144**: 3957–3967. DOI: 10.1021/jacs.1c12006.
- Newton, T.D., and Pluth, M.D. (2019). Development of a hydrolysis-based small-molecule hydrogen selenide (H<sub>2</sub>Se) donor. *Chem. Sci.* **10**: 10723–10727. DOI: 10.1039/C9SC04616J.
- Yang, Y., Sun, B., Zuo, S., et al. (2020). Trisulfide bond-mediated doxorubicin dimeric prodrug nanoassemblies with high drug loading, high self-assembly stability, and high tumor selectivity. *Sci. Adv.* **6**: eabc1725. DOI: 10.1126/sciadv.abc1725.
- Vestergaard, M., Bald, D., and Ingmer, H. (2022). Targeting the ATP synthase in bacterial and fungal pathogens: Beyond *Mycobacterium tuberculosis*. *J. Glob. Antimicrob. Resist.* **29**: 29–41. DOI: 10.1016/j.jgar.2022.01.026.
- Lamprecht, D.A., Finin, P.M., Rahman, M.A., et al. (2016). Turning the respiratory flexibility of *Mycobacterium tuberculosis* against itself. *Nat. Commun.* **7**: 1–14. DOI: 10.1038/ncomms12393.
- Liu, Z., Guo, K., Yan, L., et al. (2023). Janus nanoparticles targeting extracellular polymeric substance achieve flexible elimination of drug-resistant biofilms. *Nat. Commun.* **14**: 5132. DOI: 10.1038/s41467-023-40830-9.

## ACKNOWLEDGMENTS

This work was supported by the National Natural Science Foundation of China (52273118 and 22275013) and the Fundamental Research Funds for the Central Universities (QNTD2023-01). Many thanks for the support of the Postdoctoral Fellowship Program of CPSF (GZC20230196). All animals were treated under the guides of the SPF Animal Department of Clinical Institute in China-Japan Friendship Hospital (N. Zryhy 12-20-08-3).

## AUTHOR CONTRIBUTIONS

M.L. and F.B. contributed equally. W.X., H.X. and X.W. conceived the concept and supervised the work. M.L. and F.B. performed the experiments and wrote the manuscript. G.L. were involved in the preparation of materials and the analysis of the results.

## DECLARATION OF INTERESTS

The authors declare no competing interests.

## SUPPLEMENTAL INFORMATION

It can be found online at <https://doi.org/10.59717/j.xinn-life.2024.100076>

## LEAD CONTACT WEBSITE

Wensheng Xie: [http://www.wangxing-lab.com/team\\_content.aspx?id=17199](http://www.wangxing-lab.com/team_content.aspx?id=17199)

Huaping Xu: <http://xuslab.com/about-me/>

Xing Wang: [http://www.wangxing-lab.com/team\\_content.aspx?id=4694](http://www.wangxing-lab.com/team_content.aspx?id=4694)